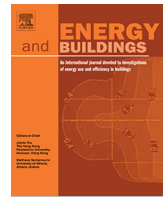




ELSEVIER

Contents lists available at ScienceDirect



Room-level load shifting of space heating in a single-family house – A field experiment

V. Amato*, R.E. Hedegaard, M.D. Knudsen, S. Petersen

Department of Civil and Architectural Engineering, Aarhus University, Inge Lehmanns Gade 10, 8000 Aarhus C, Denmark

ARTICLE INFO

Article history:

Received 1 June 2022

Revised 8 November 2022

Accepted 27 December 2022

Available online 31 December 2022

Keywords:

Energy flexibility

Demand-side management

Residential space heating

Economic model predictive control

Field experiment

ABSTRACT

Recent simulation-based studies have indicated that load shifting using Economic Model Predictive Control (E-MPC) of radiators for residential space heating can be utilized for demand response purposes in energy systems. However, there is a lack of studies on whether this load shift potential can be realized in real, inhabited buildings. This paper reports on a field experiment aiming at realizing load shifting of space heating in a single-family house with a hydronic radiator system connected to the local district heating. Radiators in a limited number of 'active' rooms were controlled using set-point schedules mimicking the typical behavior of E-MPC. The results indicate that it was possible to load shift heating consumption in the 'active' rooms but that the load shift for the building as a whole was limited due to the hydraulics of the radiator system. The paper also reports on the several practical issues encountered during the experiments – issues that in different ways are barriers to the practical realization of demand response from E-MPC of hydronic space heating systems.

© 2022 The Authors. Published by Elsevier B.V. This is an open access article under the CC BY license (<http://creativecommons.org/licenses/by/4.0/>).

1. Introduction

An increasing amount of studies have indicated a significant theoretical potential of utilizing Economic Model Predictive Control (E-MPC) of space heating systems to exploit the thermal mass in residential buildings for demand response (DR) purposes in district heating systems [1–6]. These studies assume that individual buildings in the district heating system are equipped with technology that enables E-MPC. Several simulation-based studies have demonstrated how to set up effective concepts for E-MPC of room radiators in individual buildings assuming that the required hardware and software infrastructure is available and fully functional, see e.g. [7–10] to mention a few. However, these concepts have very seldom been tested in real residential buildings [11,12]. There is consequently a lack of knowledge on whether it is possible to obtain the theoretical load shifting potential identified by simulation-based studies reported in the literature – let alone identification of any practical barriers and implications in doing so. To further advance on these issues, the study reported in this paper aimed to realize the typical variations in heating set-point of E-MPC schemes for the purpose of heat load shifting observed in previous simulation-based studies of E-MPC of radiators in space heating systems in an actual residential building. To this end, an

occupied single-family house with hydronic radiators connected to the district heating system of the city of Aarhus, Denmark, was equipped with remote-controlled thermostats, various temperature measuring equipment, and a heat meter logging heat energy use in high precision and temporal resolution. The rooms of the house were divided into an active zone, whose radiators were controlled, and a passive zone, which was not part of the experiment. The reason for excluding some rooms from the experiments was that previous studies indicated that building users prefer distinct temperatures in different rooms and, in particular, lower bedroom temperatures [13–19]. Experiments modulating the indoor air temperature in the active zone according to a set-point schedule *mimicking* the typical behavior of a real E-MPC were carried out to avoid the practical issues of implementing an actual E-MPC scheme for set-point control. The experiments were executed during the full heating season of 2020–2021, and the outcome in terms of load shifting potential was analyzed. Furthermore, the experiments led to the identification of many practical issues that need to be dealt with to obtain a robust and reliable E-MPC setup. This paper therefore also provides an overview of these issues as input to researchers interested in developing robust solutions for remote control of hydronic radiators.

The paper is divided into three main parts. Section 2 outlines the method of the study by describing the experimental idea, the case building, and the equipment installed. Section 3 provides details on the design and results of the individual experiments.

* Corresponding author.

E-mail address: viam@cae.au.dk (V. Amato).

Section 4 contains a discussion of the results and insights obtained from the experiments before conclusions are provided in **Section 5**.

2. Method

The experiments realizing typical heat load shifting behavior was conducted as a case study featuring a detached single-family house located on the outskirts of the city of Aarhus, Denmark – see section 2.1 and 2.2 for further details on the case building, and the experimental equipment and data collection, respectively.

A total of three consecutive experiments were conducted. The first experiment (Experiment 1) was designed to test whether the case house was able to provide a load shift of district heating. Previous simulation-based studies listed in the introduction have indicated that the typical behavior of E-MPC of residential space heating systems using prices from the day-ahead electricity market is that it boosts the indoor air temperature to a user-defined upper limit in a low-price period leading up to high-priced peak load situations in the energy system [20–23]. The E-MPC thereby stores low-price thermal energy in the thermal mass of the building so that the building heating system can be shut off or run at a minimum during the high-price peak period while the indoor temperature returns to the user-defined lower limit. In a Danish context, this behavior is typically seen around the hours of early morning (approx. 6–8 am) when many building occupants just have woken from their night's sleep [24,25]. It is at this time of the day when Experiment 1 reported in section 3.1 is attempting to realize set-point schedules mimicking the typical morning boost behavior of E-MPC. The effect of the different schedules was evaluated in terms of their ability to boost the indoor temperature and consequently shift heat load away from the district heating morning peak from 6 to 8 am while maintaining thermal comfort.

The scope of the second experiment (Experiment 2) was to investigate the load shifting potential of the case house throughout the day and how the E-MPC behavior affects the comfort of the residents. To this end, hourly random binary signals were generated to choose between a lower and higher comfort limit temperature set-point in each hour of the day. The experiment is reported in **Section 3.2**.

Findings from Experiment 1 and 2 led to the formulation of a third experiment; see **Section 3.3** for further details.

2.1. Case description

The study was carried out in a detached single-family house depicted in **Fig. 1** located in a suburban area of Aarhus, Denmark. The house was built in 1968 and is currently occupied by a family of four people (two adults, and two minor children). The house has a gross floor area of approximately 220 m² distributed on one floor (see **Fig. 2**) and the room height is 2.3 m. The external walls are brick cavity walls with a total width of 0.29 m whereof approx. 0.075 m is mineral wool insulation. The ground deck has a 0.022 m solid wood flooring on joists resting on a 0.08 m concrete cast on a layer of sand. The cavity between the flooring and the concrete is 0.1 m whereof 0.075 m. is mineral wool insulation. The exceptions of this ground deck build-up are the bathrooms where flooring is tiles mounted on a layer of concrete cast on top of 0.075 m insulation and the utility room next to the kitchen where tiles are mounted on a layer of 0.25 m PUR insulation. The roof consists of a ceiling cladding of 0.022 m wood or plaster mounted on the 0.1 m rafter heads with mineral wool insulation in between. An additional layer of approx. 0.3 m paper wool insulation was added in the year 2012. The original windows were replaced in 2005 with double-layer glazing in the combined aluminum and wood frames.

The hydronic heating system of the house is shown in **Fig. 3**. It is connected to the local district heating system for space heating and domestic hot water (DHW) preparation; the hydraulic connection with the space heating system is direct while DHW is prepared by a heat exchanger between the direct district heating and domestic cold water. The connection design of the radiators is parallel, and there are radiators in every room, except in the corridors (see **Fig. 2**). The supply temperature is regulated by a weather compensation control system. The district heating consumption data is metered and logged as an hourly cumulative sum of space heating and domestic hot water consumption with a resolution of 1 kWh/h.

The case house was built during a period when minimum insulation requirements in the Danish building regulations were introduced (the year 1961) and before this minimum requirement was tightened (the year 1973). The house, therefore, belongs to an archetype construction period that constitutes approx. 15 % of all detached single-family houses, approx. 10 % of the total heated area, and 12 % of the heating consumption in the district heating system of Aarhus [26–28]. The case house, therefore, represents a type of building with a significant potential for energy-related improvements.

2.2. Experimental equipment and data collection

Fig. 2 illustrates that the house was divided into 'active' (yellow) and 'passive' (blue) rooms. Only the 'active' rooms were equipped with remote-controlled thermostats (marked 'T') and room air temperature sensors (marked 'S') used for experiments outlined in Section 2.1 while the radiators in the 'passive' rooms remained manually controlled. The selection of 'active' and 'passive' rooms was based on considerations of expected load shifting potential and residents' comfort. The bedrooms and secondary rooms (guest rooms, utility rooms, bathrooms) were chosen to be 'passive' based on a dialogue with the residents. This is aligned with previous studies which indicated that household residents prefer colder temperatures in the bedroom and therefore would not accept control strategies that boost the indoor temperature [13–19]. It was accepted to 'activate' the rooms that are used the most during the daytime: The living room, the dining room, and the kitchen. The living room and the dining room are the largest rooms in the house (36 m² and 21 m², respectively) and they have a large share of the external walls. Consequently, these rooms are expected to have a significant fraction of the total heat loss of the building – a heat loss that constitutes a potential for load shifting.

The thermostats installed in the 'active' rooms were of the brand Aeotec model number ZWA021, which integrates an electrical actuator for radiator valves with an embedded controller that allows full wireless remote control using a Z-wave network (see **Fig. 3**). The thermostats are 2x AA battery-driven. The embedded controller is a PI regulation of the valve opening position to obtain and maintain a user-defined set-point temperature using an embedded temperature sensor as the control variable. The embedded controller allows for customizing an offset for the control variable e.g. to account for differences between the temperature near the thermostat and the area where the occupants normally stay in the room. A room air temperature sensor in the occupied area can be used to update this offset dynamically. It is also possible to bypass the default controller and directly control the valve opening position and thereby reducing the thermostat to an actuator. The thermostats have a temperature reading resolution of 0.1 °C and a valve opening reading resolution of 1 %. The thermostats were mounted on the supply side of the radiator as shown in **Fig. 3** except in the dining room where it was installed on the return side because of Z-wave connectivity problems. The thermostats come with various adaptors for mounting as they are designed to fit modern valves and therefore do not immediately

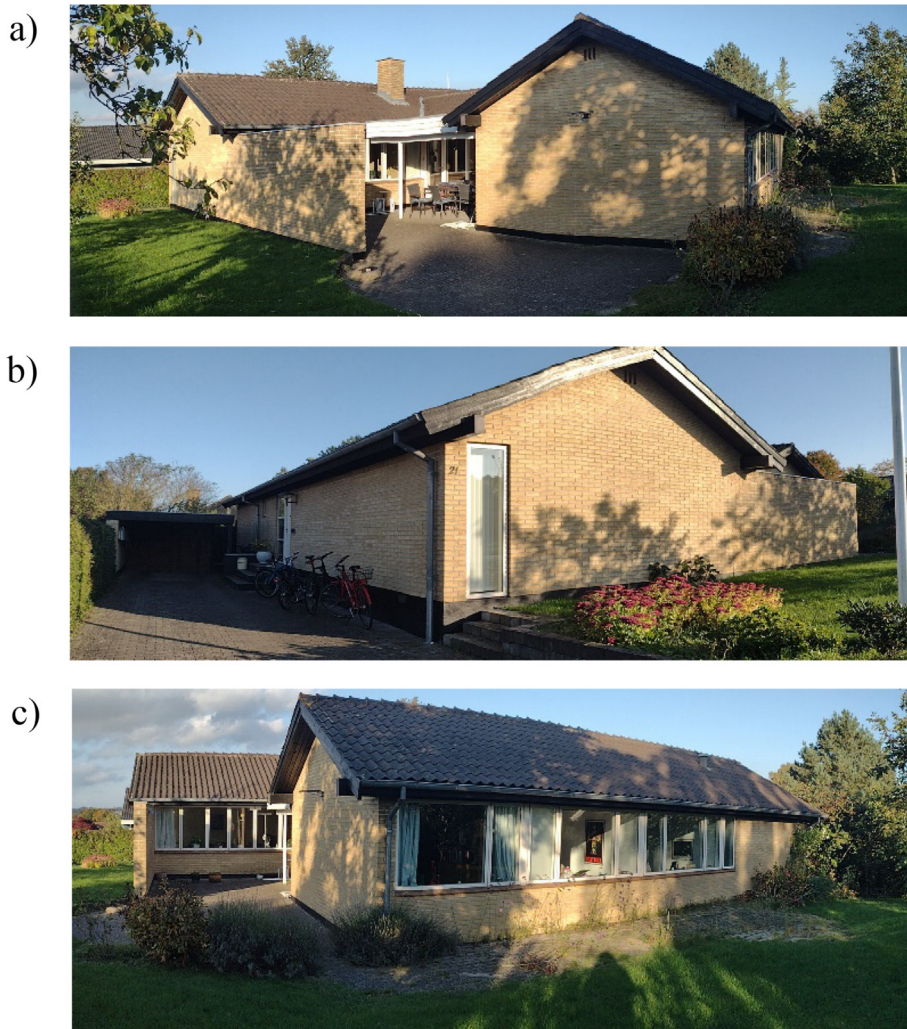


Fig. 1. Pictures of the building used as test case. a) South-west, b) North-west, c) South.

fit e.g. the existing Danfoss RAV valves of the case house. The integration of the thermostats in a Z-wave network allowed them to send and receive signals from the software Home Assistant [29] installed on a Raspberry Pi with a Z-wave stick located in one of the large utility rooms (Fig. 2). The Raspberry Pi was connected to the household wireless internet enabling control of the temperature set-points or valve opening signals remotely using MATLAB [30] or the AppDaemon [31] environment.

The sensors used for room air temperature measurements (see Fig. 2) and inlet/outlet temperature of each radiator (see Fig. 3) were of the brand HeatMoniSpot by ReMoni [32] which has an accuracy of ± 0.5 °C. Measurements were sent every 5 min through a dedicated gateway connected to the house's wireless internet to a ReMoni server. The data from the ReMoni server were transferred to the InfluxDB database [33] which was integrated into Home Assistant. The room air temperature sensors were located on the opposite side of the room away from the radiator at the height of a sitting person (1.1 m) in the living room and dining room and the height of a standing person (1.7 m) in the kitchen. A HeatMoniSpot sensor was also used for outdoor air temperature measurements in a permanently shaded outdoor location.

A heat meter of the brand Kamstrup Multical 603 [34] with a wired M–BUS was installed centrally at the district heating supply and return of the case house. The M–BUS was connected to the Raspberry Pi where the signal was stored every-five seconds. The

obtained heating data was the combined consumption for space heating and preparation of domestic hot water. The separation of domestic hot water (DHW) from space heating consumption was performed by using a modified version of the statistical time series method developed by Bacher et al. [35]. The method was modified because peaks of space heating consumption due to an increased temperature set-point were classified as peaks of DHW consumption. The modification consisted in setting the DHW consumption to 0 in the time range from 5 min before to 1 h after a set-point increase.

The residents were asked to give feedback on any discomfort experiences and practical issues during the experimental period at any time via telephone or a chat service.

3. Experiments

The following sections report on the experiments outlined in Section 2 with a focus on the load shifting potential of the case house. As mentioned in the introduction (Section 1), the experiments led to the identification of many practical issues regarded as important findings to researchers interested in developing robust solutions for the remote control of hydronic radiators. These issues are discussed in Section 4.

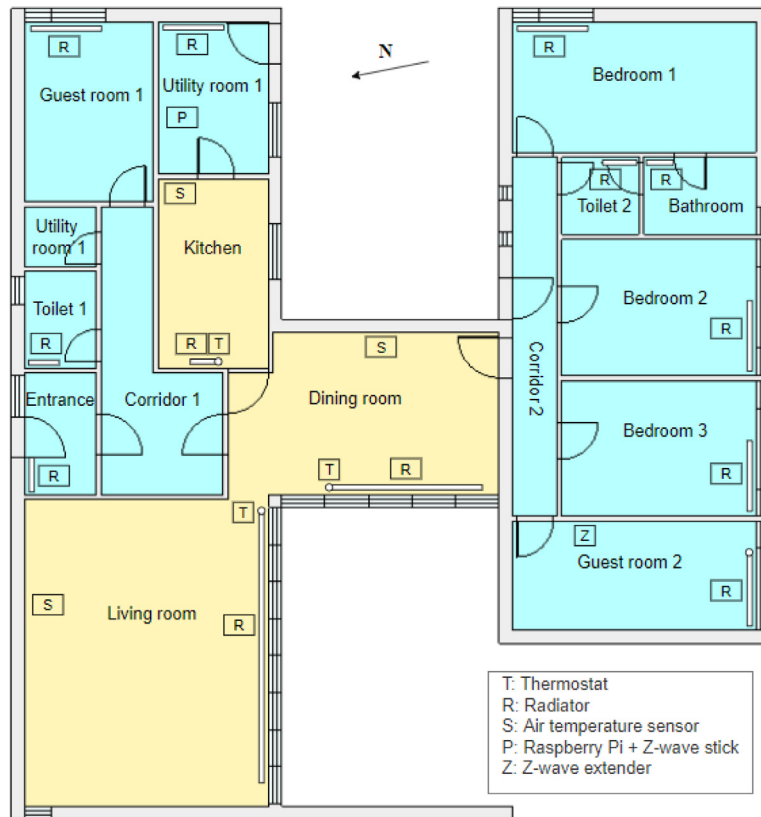


Fig. 2. Floor plan of the building and location of the experimental equipment and radiators. Yellow: Active rooms. Blue: Passive rooms. (For interpretation of the references to colour in this figure legend, the reader is referred to the web version of this article.)

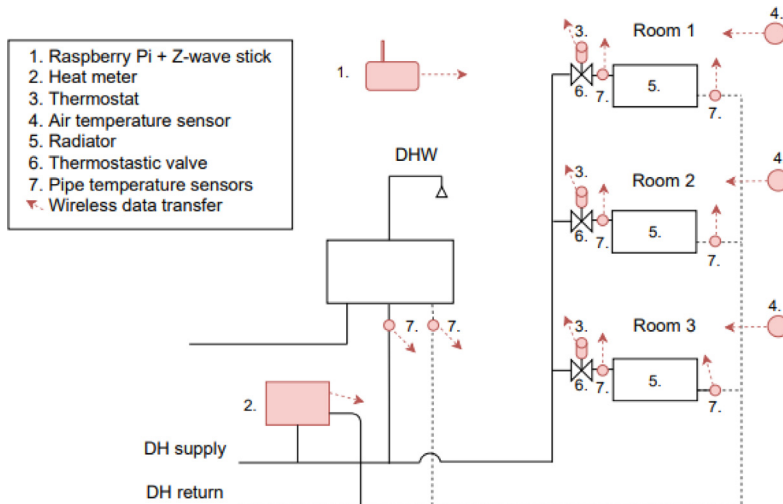


Fig. 3. Diagram of the heating system and the experimental equipment. The components installed for the experiments are colored in red, while the components already present in the building are not coloured. DH is an abbreviation of district heating. (For interpretation of the references to colour in this figure legend, the reader is referred to the web version of this article.)

3.1. Experiment 1: boosts in fixed nighttime periods using the thermostat embedded set-point control

Boost periods mimicking the typical behavior of E-MPC (as explained in the method section) were executed every second night for 18 days (from the 4th to the 22nd of December). The boost period lasted either one, three, or five hours, and always ended at 5 am. The set-point during the normal operation was set to 20 °C and the set-point for temperature boost periods was

23 °C. The set-point was tracked using the embedded controller of the thermostat. The load shifting potential was evaluated by observing how fast the temperature decayed after the end of the boost period and for how long the heat consumption was reduced after the set-point was returned to normal operation.

Initially, the embedded temperature sensor in the thermostat was used as the control variable. However, a significant discrepancy between the measurements of the embedded temperature sensor and the room temperature sensor was observed. The

embedded sensor indicated a higher temperature than the room sensor when the radiators were on, meaning that the embedded controller reached the boost set-point very quickly and the subsequent tracking of the set-point did not lead to a significant increase in the room temperature. Consequently, the temperatures decayed quickly to the normal operation set-point after the boost period. To avoid this behavior, the thermostat temperature offset was calibrated with a frequency of 10 min to match the temperature measured by the room temperature sensor. The offset was calculated as the difference between the temperature measured by the thermostat-embedded sensor and the temperature measured by the room sensor. This dynamic offset calculation was used throughout Experiment 1.

The district heating substation in the case house has a weather compensation mixing loop to control the supply temperature as a function of outdoor temperature. However, it was observed early in the study that the weather compensation during periods with mild outdoor temperatures reduced the supply temperature to a level where the available heat power was not sufficient to reach the boost temperature set-point. To avoid this issue, the weather compensation was disabled, and the supply temperature was consequently always at approximately 65 °C throughout the remaining study.

Fig. 4 shows an example of data collected during the heat boost experiments of different time duration – one, three, and five hours – using dynamic temperature offset and no weather compensation in the active zones. From **Fig. 4** (first row) it is evident that the duration of temperature decay back to the normal operating temperature after a heat boost period is proportional to the length of the heat boost period and that the decay varied in different rooms. The temperature decay after a heat boost of one hour was typically 1.5 h, and 3.5 and 6 h after longer boosts of three and five hours, respectively. The valve opening of the radiators shown in **Fig. 4** (second row) indicates that no heating was used in the rooms during the temperature decay. Exceptions were observed in the one- and three-hour heat boost of the living room, where the integral action of the thermostat-embedded controller accumulated a high control error during the heat boost led to continuous heating after the set-point was returned to normal operation. Despite this, the data shows that a typical fluctuating indoor temperature behavior observed in previous simulation-based studies of E-MPC, e.g. as in Refs. [20–23], was realized as per **Fig. 4** (first row) and that a load shift was obtained in the active zones indicated by the shut valves in **Fig. 4** (second row). However, **Fig. 4** (third row) indicate that the effect of this load shift on the overall district heating energy consumption of the house was very limited; a potential reason for this was investigated further in Experiment 3 (see section 3.3). Finally, **Fig. 4** (fourth row) indicate that preheating the rooms led to increased return temperatures at the heat meter; the cooling decreases from approx. 40–50 °C during normal operation to approximately 30 °C during the boost periods.

One adult resident of the case house using the active rooms from approx. 6 am to 7 am on weekdays reported several times that the room temperature in the active rooms often was perceived as ‘unpleasantly warm’. It is noted that the morning routine of this adult was to put on a full-body sweater after leaving the bed to avoid feeling cold when entering active rooms that were usually no more than 20 °C during normal operation. The other adult resident used the active rooms from approximately 7 am to 8 am and sometimes noticed that the rooms were ‘warmer than usual’ but did not find it uncomfortable.

3.2. Experiment 2: random boosts during the whole day using a customized valve opening control

This experiment was designed to investigate the load shifting potential of the case house during different parts of the day and how the mimicked MPC behavior affected the comfort of the residents. To this end, an hourly binary signal was used to generate a heating set-point schedule of either normal operation mode (20 °C) or temperature boost mode (22 °C). The binary signal was calculated according to the value of a random number between 0 and 1 that was generated every hour. The boost temperature was decided upon in consultation with the residents. The experiment was executed every day for 9 weeks (from the 5th of January to the 12th of March). The thermostat-embedded PI controller was substituted by a customized PI control of the valve opening position to avoid the inappropriate integral action of the embedded controller observed in Experiment 1. The valve opening was controlled as follows:

$$\text{Valveopening} = 50 + K_p \cdot \left(e + \frac{ei \cdot t_s}{t_i} \right) [\%]$$

where the proportional gain (K_p) was set to 25, the integral time (t_i) was set to 2250 s, and the sample time (t_s) was set to 120 s. The error e was the weighted sum of the temperature measured by the thermostat-imbedded sensor thermostat and the room sensor. The integral error ei was calculated by summing the value of ei of the previous sample time with the error e of the current sample time. A limit of 50 on the absolute value of the integral error ei was set to avoid excessive error accumulation. The room sensor measurement was assigned a weight factor of 90 % while the remaining 10 % was assigned to the thermostat measurement to include the effect of fast temperature changes in the area close to the radiator.

The results from a typical day of the experiments are plotted in **Fig. 5**. The first row of the figure shows that the room temperature in the active rooms was boosted according to the set-point schedule. However, the room temperatures dropped faster back to the normal operating temperature after a temperature boost than in Experiment 1 (**Fig. 5**) presumably because of lower outdoor temperatures. **Fig. 5** (second row) shows that the customized PI control closed the valves after the end of a boost thus indicating that the customized PI is more appropriate for boosting behavior than the embedded PI control used in Experiment 1. **Fig. 5** (third row) shows that the effect of the pre-heating on the overall heating energy consumption of the house is visible as the lowest levels of consumption are in the hour after the boosts; however, the effect is rather limited as in Experiment 1. **Fig. 5** (fourth row) indicates that there are spikes in the return temperature when a temperature boost is starting up and then it returns to the same level as seen during normal operation mode.

Different technical problems occurred during Experiment 2 that interrupted the experiments and in the worst case led to thermal comfort issues. **Fig. 6** depicts an example where the active zones were overheated due to the loss of internet connection to the Raspberry Pi; hence, it was not possible to send signals to the thermostats to change valve position. The same problem also occurred when the Z-wave connection from the Pi to the thermostat was lost or when the thermostat batteries were drained. Furthermore, mechanical parts of the valves sometimes got stuck and therefore did not react to control signals. These issues were often discovered by the residents reporting that the room temperatures were unacceptably warm or cold. The issues were solved as they occurred by either visiting the case house or asking the residents to perform certain actions such as restarting the internet router, Raspberry Pi, or replacing batteries in thermostats.

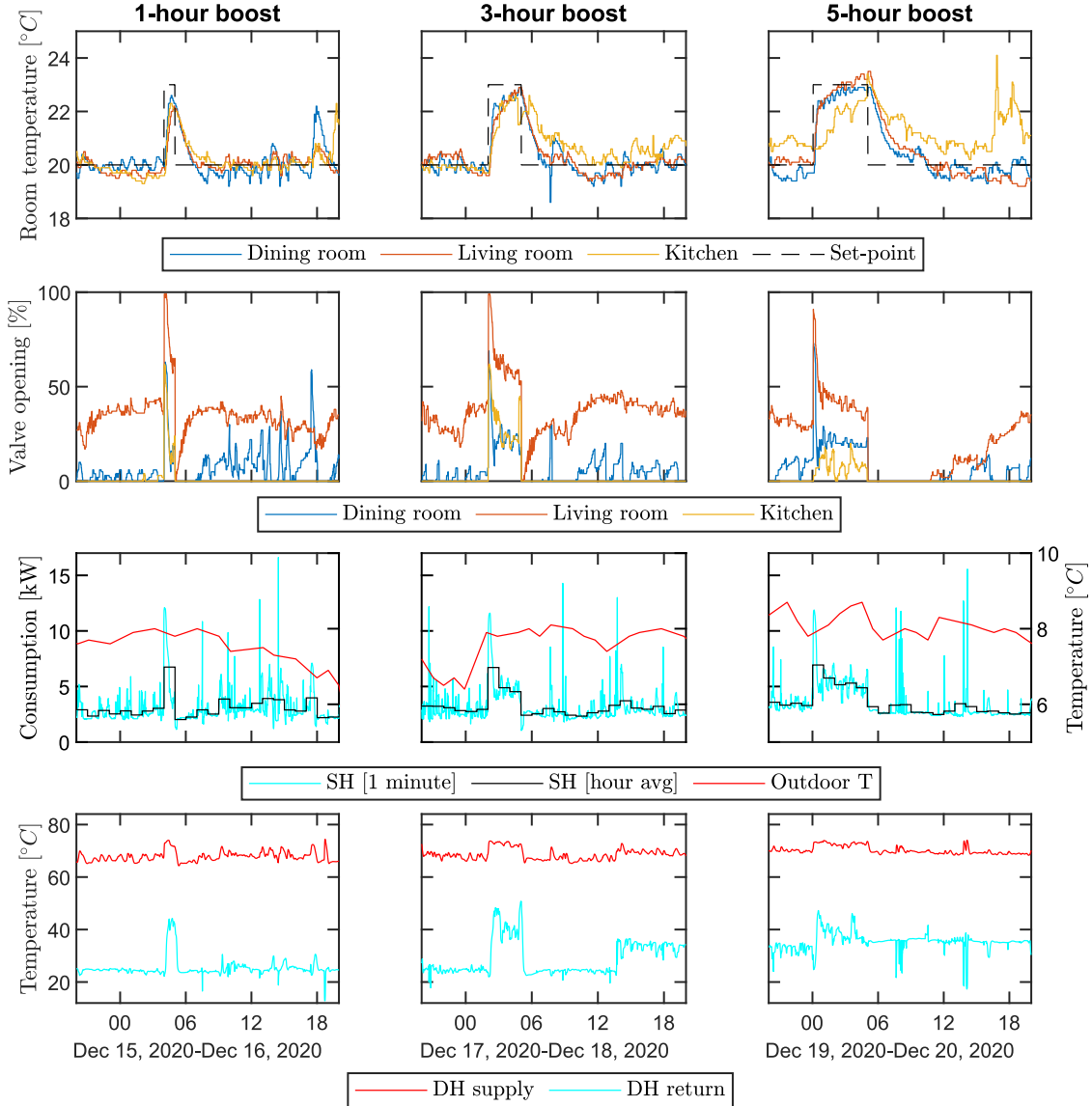


Fig. 4. Example of data from Experiment 1 for the three durations of boost periods. First row: Temperature set-points and room temperatures. Second row: Radiator valve opening. Third row: Space heating (SH) consumption and outdoor temperature. Fourth row: District heating (DH) supply and temperatures at the heat meter.

The residents did not report any thermal comfort issues during the periods with no technical problems except that they sometimes noted a remarkable warm temperature when passing areas close to the radiators. However, the residents reported that their living room radiator often became noisy right after they heard that the electronic actuator opened the valve. The noise was often observed in periods where there was little or no active space heating in the house.

3.3. Experiment 3: the influence of changes in radiator water flow in the active zone on the flow in the passive zone

Valve position data from Experiment 1 and 2 indicate that the space heating consumption was eliminated or reduced significantly at room level after a boost mimicking the behavior of an E-MPC. However, the same effect cannot be seen on the building level where the total heating energy consumption data did not show any significant load shifting for the house as a whole. The reason was hypothesized to be that all radiators of the house share the hydronic pressure provided by the district heating supplier.

Therefore, the radiators of the 'passive' rooms increased their flow just after the end of a boost in the 'active' rooms. Consequently, the heat output to the passive rooms increased and evened out the load shifts obtained in the 'active' rooms before the thermostats reacted.

The hypothesis was first tested by monitoring the radiator water flow and temperature in a 'passive' room during Experiment 2. To this end, a thermostat like the ones in the 'active' rooms was installed in the 'passive' room named *Guest room 2*, and a Z-wave network extender was installed in the room to establish a reliable signal (see Fig. 2). Furthermore, a clamp-on ultrasonic flow meter of the brand Katronic Katflow 230 capable of instant measuring and logging liquid flow in pipes with a resolution of one minute and an accuracy of 1–3 % of the measured value was installed on the single radiator in the room. Fig. 7 shows an example in the collected dataset that supports the hypothesis: A sudden increase in the radiator water flow of *Guest Room 2* was observed after the radiator valves in the active zone closed at the end of a boost even though the valve opening of the *Guest Room 2* radiator remained constant.

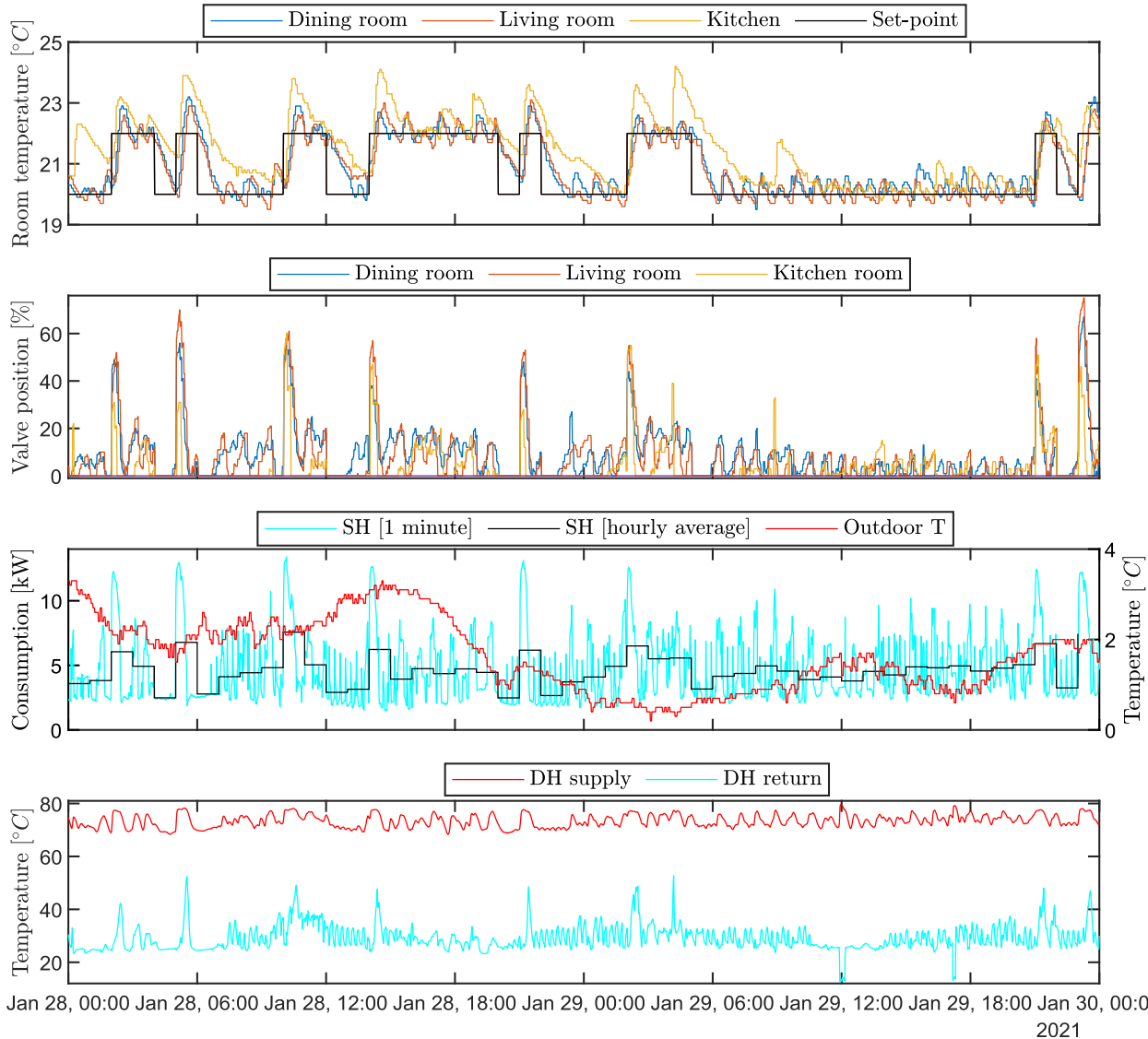


Fig. 5. Example of data from Experiment 2. First row: Temperature set-points and room temperatures. Second row: Radiator valve opening. Third row: Space heating consumption and outdoor temperature. Fourth row: District heating (DH) supply and temperatures at the heat meter.

A dedicated Experiment 3 was therefore defined to further investigate the influence of the radiator water flow in the active zone on the radiator water flow in Guest Room 2. The experiment increased the valve opening of the radiator in *Guest room 2* from fully closed to fully open by steps of 5 % every-five minutes (logging five measurements for each valve position) followed by a decrease back to fully closed using the same steps. The experiment was performed twice: One time keeping the radiator valves in the ‘active’ rooms fully closed and one time with fully open valves in the ‘active’ rooms.

Fig. 8 shows the radiator water flow as a function of the radiator valve opening during the experiments. In the experiment with fully closed valves in the ‘active’ rooms (Fig. 8, left), the water flow was approx. 10 % of the maximum value for valve openings lower than approx. 55 % and hereafter it increased steeply within a narrow range of valve opening positions ending at a flow of approx. 90 l/h at fully open. In the experiment with fully open valves in the ‘active’ rooms, (Fig. 8, right), the water flow was again approx. 10 % of the maximum value for valve openings lower than approx. 55 % but hereafter it only increased moderately – compared to Fig. 8 (left) – ending at a flow of approx. 35 l/h at fully open. The available water

flow in ‘passive’ *Guest room 2* is thus highly influenced by the valve positions in the ‘active’ rooms and is probably the reason for the increase in flow seen in Fig. 7. Overall, the experiments indicate that the hypothesized reason for why the boosts of ‘active’ rooms did not lead to any significant load shift on the building level is plausible.

4. Discussion

The results from the experiments show that it is possible to realize a load shift on zone level in a real house but also that several practical issues need to be dealt with to obtain a robust and reliable E-MPC setup. Some of the issues have already been described in section 3, such as loss of internet connection, drained batteries, and mechanical malfunction of valves. However, the experiments led to the identification of several other practical issues that had to be dealt with; this section present and discusses these. Furthermore, considerations of the overall conceptual idea tested in the experiments are also discussed.

Table 1 describes and discusses the practical issues that were encountered during the experiments followed by a short descrip-

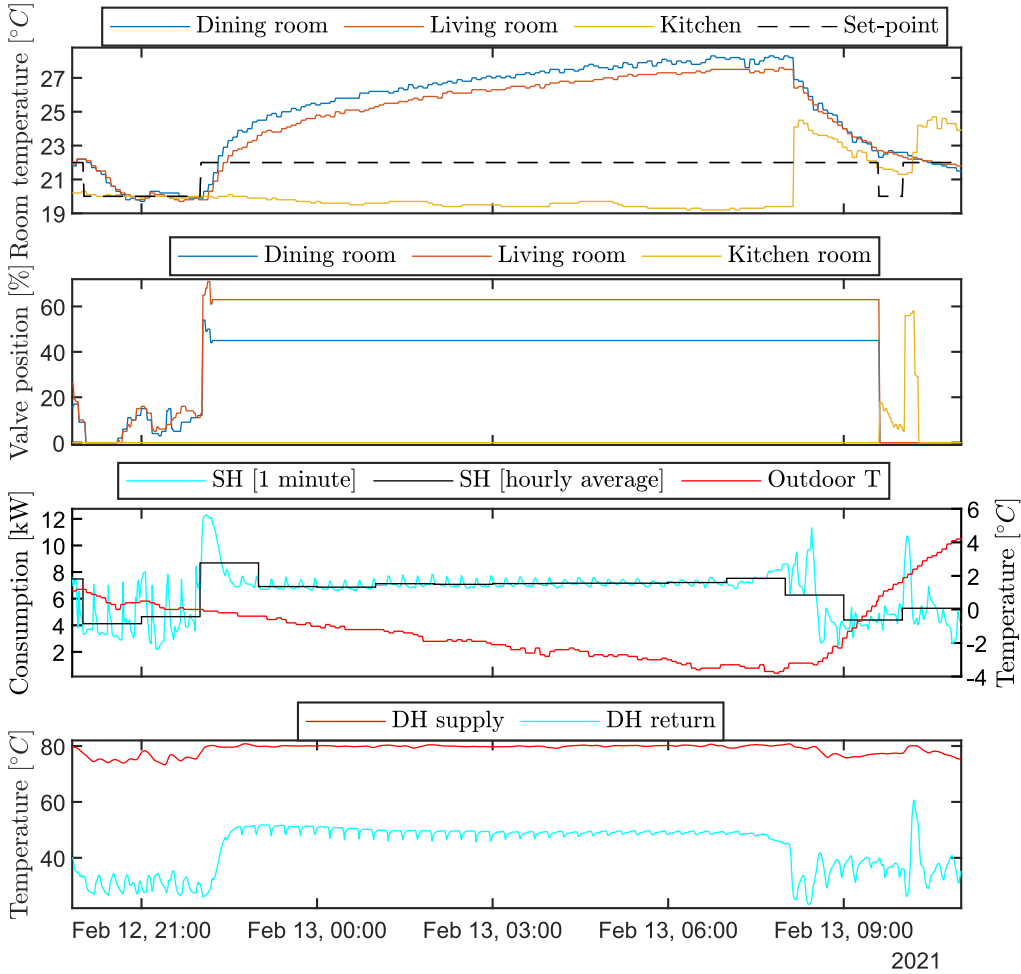


Fig. 6. Example of overheating in the active zones due to loss of internet connection to the Raspberry Pi. First row: Temperature set-points and room temperatures. Second row: Radiator valve opening. Third row: Space heating (SH) consumption and outdoor temperature. Fourth row: District heating (DH) supply and temperatures at the heat meter.

tion of potential solutions that could be further investigated in subsequent studies.

Some of the issues listed in Table 1 are pointing to challenges to the overall conceptual idea for a room-based E-MPC tested in the experiments, i.e. obtaining load shift for the house as a whole by controlling a limited amount of 'active' rooms. The concept was based on the assumption that the heat consumption was near-static in the 'passive' rooms during the heat boosts in the 'active' zones and that the load shift from the heat boosts therefore would manifest itself on the heat metering for the house as a whole. However, this was not the case; the heat boosts were counteracted by the hydraulics of the parallel-connected radiator system – a mechanism explained in Table 1. Potential solutions to the issue have been outlined in Table 1 but another solution could be to modify the conceptual idea. One modification could be to install remotely controlled thermostats in all rooms enabling the whole house to be an 'active' contributor in load shifting boosts. This will increase the cost of equipment and may lead to thermal discomfort in some rooms, e.g. bedrooms, but also open for the possibility of individual E-MPC schemes on room level – i.e. another strategy than using a common E-MPC scheme for several or all 'active' rooms as reported in this paper. An example of an individual scheme could be that bedrooms are active during the day-time and not during nighttime. However, an individual E-MPC scheme on room level requires knowledge of the heat output in the specific room. To realize this, future studies are needed to investigate how this can be obtained

with a minimum of equipment, e.g. temperature sensors on radiator supply and return pipes.

The study presented in this paper investigates a few out of many issues that are potential barriers to realising the theoretical potential of E-MPC in practice. The main issue includes how to obtain a sufficiently precise building energy simulation model for the E-MPC scheme, how to deal with forecast uncertainties (weather, energy price, occupant behavior), and how to ensure occupant comfort during temperature transitions. It is considered out of scope for this paper to further outline these issues; however, the referenced literature in the introduction of this paper indicates that several simulation-based studies have pointed to solutions for some of the mentioned issues while practical field experiments attempting to realize them are rare.

5. Conclusions

The study reported in this paper aimed to demonstrate that it is possible to obtain a load shift in heating energy use for a single-family house through E-MPC of radiators in a limited amount of 'active' rooms. The results from experiments imposing typical heat boost behavior of E-MPC indicate that the heat load was shifted in the 'active' rooms. However, these load shifts had a limited effect on the heat consumption of the house as a whole because the hydronic dynamics of the parallelly connected radiators in the 'active' and the 'passive' rooms (rooms with no heat boosts) counter-

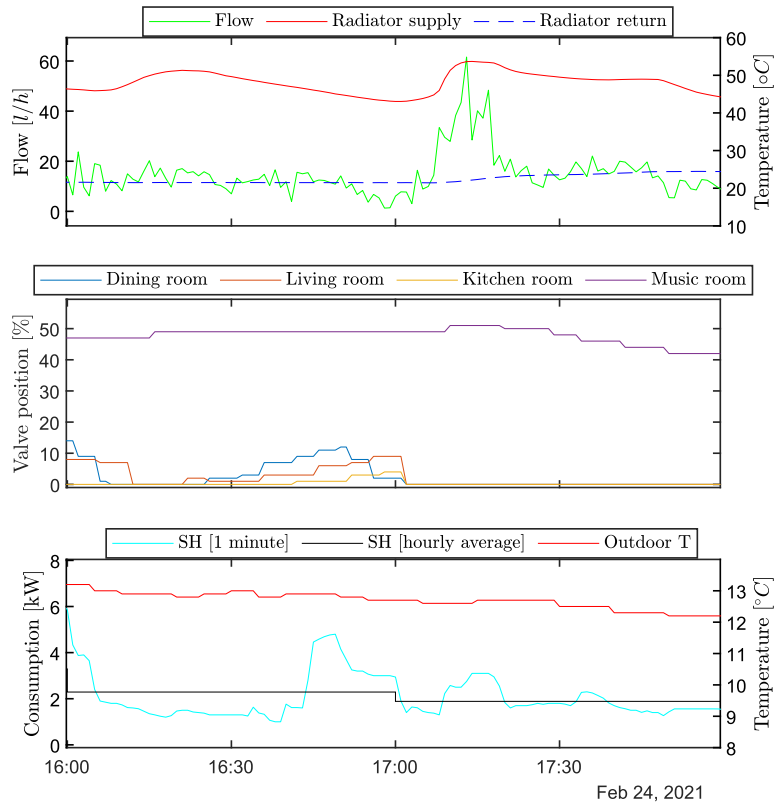


Fig. 7. Example of data from Experiment 2 that substantiate the hypothesis of an interaction between the water flow of different radiators. Top: Radiator water flow and temperatures in Guest Room 2. Middle: Radiator valve opening. Bottom: Space heating (SH) consumption and outdoor temperature.

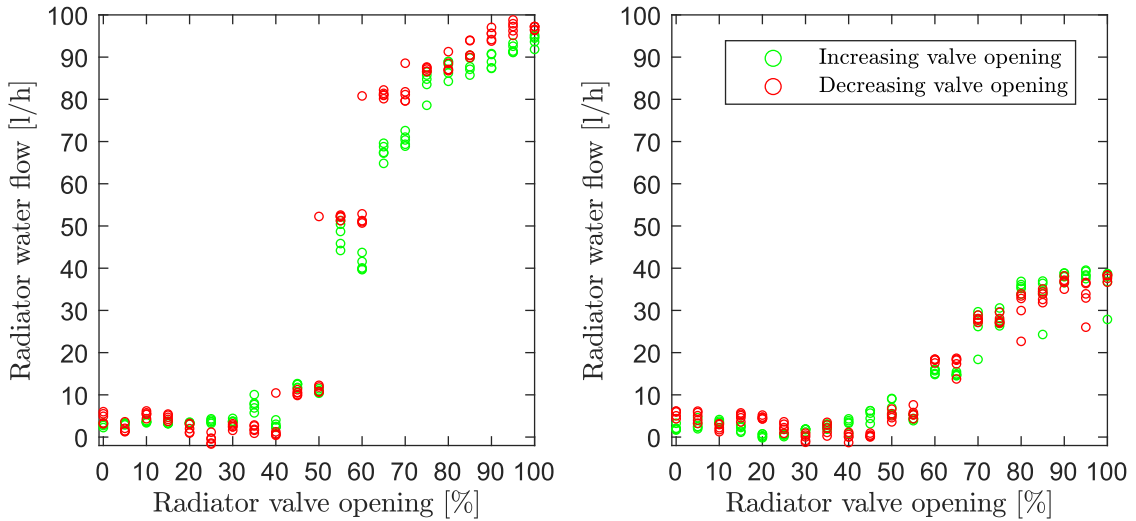


Fig. 8. Radiator water flow as a function of radiator valve positions in Guest room 2. Left: No radiator water flow in the 'active' rooms (radiator valves fully closed). Right: Maximum possible radiator water flow in the 'active' rooms (radiator valves fully open).

acted the load shifts. This suggests that the conceptual idea of obtaining a heat load shift of a house by E-MPC of a limited amount of radiators to obtain demand response, e.g. mitigation of peak loads in district heating systems, may not be appropriate; see the discussion section for proposals for a discussion of alternative concepts and their implications.

Table 1 lists a range of practical issues encountered during the experiments reported in this paper – issues that in different ways are barriers to the practical realization of demand response from E-MPC of hydronic space heating systems. This outcome of the exper-

iments is considered to be useful to researchers and product developers interested in developing – not only robust and reliable E-MPC setups – but any control systems based on wireless remotely controlled thermostats for hydronic radiators.

Data availability

Data will be made available on request.

Table 1

Description and discussion of practical issues encountered during the experiments and suggestions for how to solve them.

Issue	Description	Potential solutions
Mounting modern thermostats on old radiator valves	The thermostat used in this experiment comes with a set of adaptors as it does not fit the thread of old Danfoss valves (RA, RAV, and RAVL). The radiators of the case house had RAV valves. The RAV adaptor comes with a plastic pin that must be plugged into the valve tappet. This pin had to be modified carefully in length to be registered by the thermostat using a pincer and sandpaper.	Development of a better adaptor system for RAV valves. A more expensive solution would be to replace the valves with modern ones.
Radiator valve tappet getting stuck	A problem encountered especially during Experiment 2 was that the valve tappet got stuck in an open position even though the valve tappet position was registered as closed by the thermostat. This led to severe overheating.	Implementation of a 'valve exercise algorithm' that performs a release/push routine of the valve tappet when certain conditions are registered in data and/or according to a fixed periodical schedule.
Noise from radiator pipes caused by water flow	The residents reported that the radiator in the living room sometimes was rather noisy. They also reported that the noise was reduced when domestic hot water was tapped simultaneously e.g. in the kitchen. The problem thus arises at a certain local pipe pressure. This issue is not directly linked to the experiments, but the variable set-points increased the noise incidents.	This issue is difficult to deal with as it is difficult to pinpoint where the noise precisely is coming from. It could be due to the layout or state of the piping or the radiator valve – or a combination.
Occasional overheating of the area close to the radiators in the active rooms	The residents sometimes noted a remarkable warm temperature when passing areas close to the radiators. This was probably because of a high supply temperature to the radiators which was not weather compensated to maximize the available power during boosting.	Reduce the supply temperature which consequently will increase the flow.
High return temperature from the radiators	Data from the experiments show that boost periods can lead to high return temperatures. A low return temperature is currently an important issue for many district heating operators to ensure high system efficiency. However, future conditions may be that energy flexibility in some situations is more desirable than low return temperature.	A better balance between the desire for temperature boosts and a low return temperature from radiators can probably be obtained by customization of the radiator heating set-point.
Hydraulic balance of radiator system	The experiments show that the valve tappet position of the individual radiator affects the available water flow for other radiators in the house. This resulted in a decreased flow in the 'passive' rooms during boosts in the 'active' rooms, and increased flow in the 'passive' rooms immediately after the boost ended in the 'active' rooms – a behavior that counteracted the expected load shifting effect from the boosts for the house as a whole.	Change the setpoint in the 'active' zones incrementally while using PI thermostats in the 'passive' zones. An alternative is to install a pump centrally in the heating system that ensures constant available pressure in the radiator system.
Battery life	The AA batteries of the thermostats in the 'active' zones needed to be replaced several times throughout the experiments as the batteries were drained by the relatively frequent thermostat regulation. This was especially the case in Experiment 2 which employed a valve opening control strategy. Drained batteries in this experiment resulted in a locked position of the valve tappet with an increased risk of too low or – especially in the case of batteries drained in the middle of a boost – indoor air temperature way above the temperature set point.	Wired electricity to the thermostats is a possible but also expensive and intrusive solution. Increase battery lifetime by defining a control strategy with less frequent need for mechanical regulation of valve position. Use thermostats with a wax or gas motor to avoid temperatures above or below desired temperature set point.
Stable internet and Z-wave connection	Internet connection for the Raspberry Pi and a Z-wave signal for all the thermostats was sometimes lost making it impossible to send new signals to the thermostats. This could lead to the same indoor temperature problems as described under the issue 'Battery life' when using the valve opening control strategy.	Better positioning of Z-wave dongle and extenders. Use the embedded set-point temperature control instead of the valve opening control strategy. As under the issue 'Battery life', use thermostats with wax or gas motor. Repeating experiments with separated measurements of space heating and domestic hot water consumption. The precision of the statistical method could be refined by using temperature measurements from a sensor placed on the outgoing pipe from the domestic hot water heat exchanger to determine if domestic hot water is tapped or not.
Separation of domestic hot water consumption	The heat consumption data commonly available in Danish residential buildings are hourly truncated data with a resolution of 1 kWh of the total heating energy consumption, i.e. no separation of energy use for space heating and domestic hot water. Separating the two consumptions using statistical methods has been attempted but a higher resolution of data is needed to improve the precision of these methods [36]. In this experiment, the resolution of the heating consumption measurement was increased to 0.1 kWh/h and the space heating consumption was separated using a statistical method; however, the precision of the approach was not validated. It could also be that the statistical method could be improved if using additional data.	Defining a control algorithm that relies on offsets of the setting of the thermostat temperature set point defined by residents. This could also reduce investment costs as it makes a room temperature sensor obsolete.
Room air temperature	There were significant differences between the temperature measured by the thermostat and the temperature measured by the room temperature sensors. This is a well-known issue and the reason why traditional analog radiator thermostats e.g. Danfoss do not have a temperature scale but a simple numeric scale e.g. 1–5.	Investigations of appropriate PI settings of the thermostat for temperature boosts. Use thermostats with a wax motor instead of an electronic PI control.
Tuning of PI control	The boost performance improved from Experiment 1 to Experiment 2 due to the valve position control strategy with customized PI control. Note the problems with this control strategy explained under the issues 'Battery life' and 'Stable internet and Z-wave connection'.	

Declaration of Competing Interest

The authors declare that they have no known competing financial interests or personal relationships that could have appeared to influence the work reported in this paper.

Acknowledgements

The study was conducted as a part of the project PreHeat funded by EUDP (Jour. No. 64019-0127)

References

- [1] H. Cai, C. Ziras, S. You, R. Li, K. Honoré, H.W. Bindner, Demand side management in urban district heating networks, *Appl. Energy* 230 (May) (2018) 506–518, <https://doi.org/10.1016/j.apenergy.2018.08.105>.
- [2] D. Vanhoudt, B.J. Claessens, R. Salenbien, J. Desmedt, An active control strategy for district heating networks and the effect of different thermal energy storage configurations, *Energy Build.* 158 (Jan. 2018) 1317–1327, <https://doi.org/10.1016/j.enbuild.2017.11.018>.
- [3] J. Le Dréau, P. Heiselberg, Energy flexibility of residential buildings using short term heat storage in the thermal mass, *Energy* 111 (Sep. 2016) 991–1002, <https://doi.org/10.1016/j.energy.2016.05.076>.
- [4] D.F. Dominković, P. Giannou, M. Münster, A. Heller, C. Rode, Utilizing thermal building mass for storage in district heating systems: Combined building level simulations and system level optimization, *Energy* 153 (Jun. 2018) 949–966, <https://doi.org/10.1016/j.energy.2018.04.093>.
- [5] R.E. Hedegaard, M.H. Kristensen, T.H. Pedersen, A. Brun, S. Petersen, Bottom-up modelling methodology for urban-scale analysis of residential space heating demand response, *Appl. Energy* 242 (March) (2019) 181–204, <https://doi.org/10.1016/j.apenergy.2019.03.063>.
- [6] R. E. Hedegaard, L. Friedrichsen, J. Tougaard, T. Mølbak, and S. Petersen, "Building energy flexibility as an asset in system-wide district heating optimization models," 2020, [Online]. Available: <https://39e38bfc8bfe017f9f2d17df1-16003.sites.k-hosting.co.uk/uSIM2020//Papers/Session%20B/2.%20Petersen.pdf>.
- [7] T.Q. Péan, J. Ortiz, J. Salom, Impact of demand-side management on thermal comfort and energy costs in a residential nZEB, *Buildings* 7 (2) (2017) 1–19, <https://doi.org/10.3390/buildings7020037>.
- [8] G. Reynders, T. Nuyttens, D. Saelens, Potential of structural thermal mass for demand-side management in dwellings, *Build. Environ.* 64 (2013) 187–199, <https://doi.org/10.1016/j.buildenv.2013.03.010>.
- [9] T. Johnsen, K. Taksdal, J. Clauß, X. Yu, L. Georges, S.I. Tanabe, H. Zhang, J. Kurnitski, M.C. Gameiro da Silva, I. Nastase, P. Wargocki, G. Cao, L. Mazzarella, C. Inard, Influence of thermal zoning and electric radiator control on the energy flexibility potential of Norwegian detached houses, *E3S Web Conf.* 111 (2019) 06030.
- [10] T.H. Pedersen, R.E. Hedegaard, K.F. Kristensen, B. Gadgaard, S. Petersen, The effect of including hydronic radiator dynamics in model predictive control of space heating, *Energ. Build.* 183 (2019) 772–784, <https://doi.org/10.1016/j.enbuild.2018.11.015>.
- [11] A. Kathirgamanathan, M. De Rosa, E. Mangina, D.P. Finn, Data-driven predictive control for unlocking building energy flexibility: A review, *Renew. Sustain. Energy Rev.* 135 (2021) 110120.
- [12] M.D. Knudsen, L. Georges, K.S. Skeie, S. Petersen, Experimental test of a black-box economic model predictive control for residential space heating, *Appl. Energy* vol. 298, no. February (2021), <https://doi.org/10.1016/j.apenergy.2021.117227>.
- [13] M. Berge, J. Thomsen, H.M. Mathisen, The need for temperature zoning in high-performance residential buildings [Online]. Available: *J. Hous. Built Environ.* 32 (2) (2017) 211–230. <https://www.jstor.org/stable/44>.
- [14] J. Thomsen, L. Gullbrekken, S. Grynnning, and J. Holme, *Evaluering av boliger med lavt energibehov (EBLE)*, vol. 43. 2017.
- [15] S.P. Larsen, H. Johra, User engagement with smart home technology for enabling building energy flexibility in a district heating system, *IOP Conf. Ser.*
- [16] P. Strøm-Tjejsen, S. Mathiasen, M. Bach, and S. Petersen, "The effects of bedroom air quality on sleep and next-day performance," *Proceedings for Indoor Air 2016: The 14th international conference of Indoor Air Quality and Climate*, vol. 26, no. 5 pp. 679–686, 2016, doi: 10.1111/ina.12254.
- [17] S. Hagejärd, G. Dokter, U. Rahe, P. Femenias, My apartment is cold! Household perceptions of indoor climate and demand-side management in Sweden, *Energy Res. Soc. Sci.* 73 (2021), <https://doi.org/10.1016/j.erss.2021.101948>.
- [18] P.V.K. Andersen, S. Georg, K. Gram-Hanssen, P.K. Heiselberg, A. Horsbøl, K. Johansen, H. Johra, A. Marszal-Pomianowska, E.S. Møller, Using residential buildings to manage flexibility in the district heating network: Perspectives and future visions from sector professionals, *IOP Conf. Ser. Earth Environ. Sci.* 352 (1) (2019) 012032.
- [19] L. Christensen, T. H. Broholt, and S. Petersen, "Are bedroom air temperatures affected by temperature boosts in adjacent rooms?," *CLIMA 2022 - Proceedings of the 14th HVAC World Congress*, 2022.
- [20] R.E. Hedegaard, T.H. Pedersen, S. Petersen, Multi-market demand response using economic model predictive control of space heating in residential buildings, *Energy Build.* 150 (2017) 253–261, <https://doi.org/10.1016/j.enbuild.2017.05.059>.
- [21] T.H. Pedersen, R.E. Hedegaard, M.D. Knudsen, S. Petersen, Comparison of centralized and decentralized model predictive control in a building retrofit scenario, *Energy Proc.* 122 (2017) 979–984, <https://doi.org/10.1016/j.jegpro.2017.07.456>.
- [22] T.H. Pedersen, R.E. Hedegaard, S. Petersen, Space heating demand response potential of retrofitted residential apartment blocks, *Energy Build.* 141 (2017) 158–166, <https://doi.org/10.1016/j.enbuild.2017.02.035>.
- [23] M.D. Knudsen, S. Petersen, Demand response potential of model predictive control of space heating based on price and carbon dioxide intensity signals, *Energy Build.* 125 (2016) 196–204, <https://doi.org/10.1016/j.enbuild.2016.04.053>.
- [24] M. D. Knudsen, R. E. Hedegaard, T. H. Pedersen, and S. Petersen, "Model Predictive Control of Space Heating and the Impact of Taxes on Demand Response: A Simulation Study," in *CLIMA 2016 - Proceedings of the 12th REHVA World Congress*, 2016, vol. 10, [Online]. Available: http://vbn.aau.dk/files/233817813/paper_622.pdf.
- [25] M.H. Christensen, R. Li, P. Pinson, Demand side management of heat in smart homes: Living-lab experiments, *Energy* 195 (2020), <https://doi.org/10.1016/j.energy.2020.116993>.
- [26] "Statistics Denmark, BYGB40: Buildings and their heated area by unit, time, region and type of heating." [Online]. Available: <https://www.statistikbanken.dk/BYGB40>.
- [27] M.H. Kristensen, S. Petersen, District heating energy efficiency of Danish building typologies, *Energy Build.* 231 (2021), <https://doi.org/10.1016/j.enbuild.2020.110602>.
- [28] M. Kristensen, District heating energy efficiency of Danish building typologies: Datasets and supplementary materials, *Mendeley Data* (2020). <https://doi.org/10.17632/v8nwwy7p6r.1>.
- [29] "Home Assistant." [Online]. Available: <https://www.home-assistant.io/>.
- [30] Mathworks, "MATLAB R2020b," 2020.
- [31] "AppDaemon." [Online]. Available: <https://appdaemon.readthedocs.io/en/latest/index.html>.
- [32] ReMoni, "HeatMoniSpot." [Online]. Available: <https://www.remoni.com/products2/product-overview/heatmonispot/>.
- [33] Influxdata, "InfluxDB." [Online]. Available: <https://www.influxdata.com/products/influxdb/>.
- [34] Kamstrup, "MULTICAL 603." [Online]. Available: <https://www.kamstrup.com/en-en/heat-solutions/meters-devices/meters/multical-603>.
- [35] P. Bacher, P.A. de Saint-Aubain, L.E. Christiansen, H. Madsen, Non-parametric method for separating domestic hot water heating spikes and space heating, *Energy Build.* 130 (2016) 107–112, <https://doi.org/10.1016/j.enbuild.2016.08.037>.
- [36] R.E. Hedegaard, M.H. Kristensen, S. Petersen, J. Kurnitski, T. Kalamees, Experimental validation of a model-based method for separating the space heating and domestic hot water components from smart-meter consumption data, *E3S Web Conf.* 172 (2020) 12001.